Compressing Electrical Power Grids

Zhifang Wang
Information Trust Institute
University of Illinois at Urbana-Champaign
Urbana, IL 61801
Email: zfwang@illinois.edu

Anna Scaglione
Electrical and Computer Engineering
University of California
Davis, CA 95616
Email: ascaglione@ucdavis.edu

Robert J. Thomas
Electrical and Computer Engineering
Cornell University
Ithaca, NY 14850
Email: rjt1@cornell.edu

***Abstract*—In this paper we apply the Singular Value Decomposition (SVD) analysis to examining the coupling structure of an electrical power grid in order to highlight opportunities for reducing the network traffic, by identifying what are the salient data that need to be communicated between parts of the infrastructure to apply a control action. Our main finding is that typical grid admittance matrices have singular values and vectors with only a small number of strong components. The SVD sparsity can be exploited to construct an efficient decentralized system-wide monitoring and control architecture. We also discuss the potential applications of the proposed architecture and its robustness under contingency; and experiment the SVD analysis with the NYISO-2935 system and the IEEE-300 system.**

I. Introduction

The past decade has seen many efforts to achieve a *Smart Grid*, that is, using digital technology to save energy, reduce cost and increase reliability and transparency.

However, in reality it is difficult to realize system-wide real-time monitoring and controls. The reason lies in two aspects: first, the system size is large, electrical power grids have grown into one of the largest interconnect systems which may contain thousands or even millions of buses, lines, and generation and loads; second, the delay introduced by the current centralized monitoring or measuring architecture (SCADA) is intolerable. There are two aspects in containing the cost of the sensing infrastructure: one is deploying the least amount of sensors; the other is minimizing the information that needs to flow from one section of the network to the other. The aim of our work is to examine if the coupling of the physical infrastructure highlights opportunities for reducing the network traffic, by identifying what are the salient data that need to be communicated between parts of the infrastructure.

In this paper, we apply Singular Value Decomposition analysis to examine the coupling structure of an electrical power grid. Our main finding is that typical grid admittance matrices have singular values and vectors with only a small number of strong components. The SVD sparsity can be utilized to determine what parts of the system are more strongly coupled.

The singular value decomposition (SVD) is an important factorization of a two-dimension matrix which has a huge number of applications. Researchers have been using it in electric power grid analysis and in other areas as well. For example, Tiranuchit and Thomas (1988) proposed in [1] the minimum singular value of the Jacobian matrix of an electrical power grid as a voltage security index to monitor how close a power system is operating to a voltage instability. Ekwue, Wan, and *et al.* (1999) applied an SVD method of voltage stability analysis to calculating voltage stability index, identifying the most weakest buses and areas, and ranking transmission lines. [2] in the UK National Grid system. Li (2000) utilized the SVD method to analyze electricity-demand data in a power grid and developed appropriate mathematical models and algorithms to forecast the electric demands in [3]. Janik, Rezmer, and *et al.* (2009) presented in [4] an approach based on SVD to accurate estimate of harmonic current components in a power grid network which incorporates wind generation. Krause, Lehnhoff, and *et al.* (2009) studied the operational limitation problems in a power grid with widely dispersed renewable energy sources in order to avoid voltage band violations and line overloads [5]. The authors introduced an extension multi-agent algorithm, which employed an SVD of the grid's line admittance matrix Y_{line}, to verify the feasibility boundaries in constant and predetermined time.

To the best of our knowledge, this paper is the fist effort to apply the SVD analysis to examining the coupling structure of an electrical power grid in order to guide the design of the information flow for system-wide monitoring and control.

The rest of the paper is organized as follows: Section II presents the system model for electrical power grid operation and the SVD of the network admittance matrix Y; Section III investigates a decentralized monitoring and control architecture based the compressed system model; Section IV discuss the potential applications of the proposed architecture and its robustness under contingency; Section V experiments the SVD analysis with the NYISO-2935 system and the IEEE-300 system; and Section VI concludes the paper.

II. System Model

The network equations that couple the power grid dynamics are

$$YV = I, \tag{1}$$

where $V = \mathrm{V}\angle V$ and $I = \mathrm{I}\angle I$ are the complex phasor vectors, associated to the sinusoids of instantaneous bus voltages and injected currents at the frequency $f_0 = 60$ or 50 Hz, $v(t) = \sqrt{2}\mathrm{V}\cos(2\pi f_0 t + \angle V)$, and $i(t) = \sqrt{2}\mathrm{I}\cos(2\pi f_0 t + \angle I)$ respectively. Y is the network admittance matrix at the frequency equal to f_0, which is determined not only by the connecting topology but also its electrical parameters. Given a

network with n nodes and m links (which may also be referred to as *buses and branches or lines* in power grid analysis; or *vertices and edges* in graph theory and network analysis), each link $l = (s,t)$ between nodes s and t has a line impedance $z_{pr}(l) = r(l) + jx(l)$, where $r(l)$ is the resistance and $x(l)$ the reactance. The line admittance is obtained from the inverse of its impedance, i.e.,

$$y_{pr}(l) = g(l) + jb(l) = 1/z_{pr}(l) \tag{2}$$

Then the line-node incidence matrix A, with size $m \times n$, can be formulated as

$$A : \begin{cases} A(l,s) = & 1 \\ A(l,t) = & -1 \\ A(l,k) = & 0 \text{ , with } k \neq s \text{ or } t, \end{cases} \tag{3}$$

with $l = 1, 2, \cdots, m$. The Laplacian matrix L of the network is

$$L = A^T A. \tag{4}$$

The network admittance matrix Y of the network is

$$Y = A^T diag(\mathbf{y_{pr}}) A \tag{5}$$

where $\mathbf{y_{pr}}$ is the line admittance vector. The entries in Y are as follows:

$$Y(s,t) := \begin{cases} -y_{pr}(s,t), & \text{if } t \neq s \text{ and a link } (s,t) \text{ exists} \\ \sum_{t \neq s} y_{pr}(s,t), & \text{if } t = s \\ 0, & \text{otherewise,} \end{cases} \tag{6}$$

with $s, t = 1, 2, \cdots, n$. Note that, by construction, Y is symmetric, $Y = Y^T$.

The network admittance matrix Y of an electrical power grid is usually very sparse. [6] has pointed out that the average node degree of an electrical power grid does not scale as network size increases and that its algebraic connectivity decreases as $\lambda_2(L) \propto n^{-1.376} \sim n^{-1.0604}$, lying between those of 1-D lattice and 2-D lattice. The sparsity of the coupling structure in a power grid can be also revealed by computing the SVD of Y:

$$Y = \mathbb{U} \Sigma \mathbb{V}^H \tag{7}$$

where $\mathbb{U} = \{\boldsymbol{u}_1, \boldsymbol{u}_2, \cdots, \boldsymbol{u}_n\}$ and $\mathbb{V} = \{\boldsymbol{\nu}_1, \boldsymbol{\nu}_2, \cdots, \boldsymbol{\nu}_n\}$ are unitary matrices whose column vectors are called the left and right singular vectors respectively, and Σ is a diagonal matrix with the non-negative singular values ordered by magnitude, $\{\sigma_1 \geq \sigma_2 \geq \cdots \geq \sigma_n = 0\}$. And (7) can be expressed as

$$Y = \sum_{k=1}^{n} \sigma_k \boldsymbol{u}_k \boldsymbol{\nu}_k^H. \tag{8}$$

Since the matrix Y is symmetric, it can be proved that there exists a decomposition satisfying that $\mathbb{U} = \mathbb{V}^*$. Accordingly, for each pair of the singular vectors, we have $\boldsymbol{u}_k = \boldsymbol{\nu}_k^*$. [1]

It is well known that, when there are $w (\ll n)$ dominant singular values (vectors), the matrix admits a low rank approximation:

$$Y \approx \widetilde{Y} = \sum_{k=1}^{w} \sigma_k \boldsymbol{u}_k \boldsymbol{\nu}_k^H. \tag{9}$$

The approximation error of (9) can be measured by the normalized Frobenius norm, that is,

$$e_w = \|Y - \widetilde{Y}\|_F = \left(\sum_{k=w+1}^{n} \sigma_k^2 \right) / \left(\sum_{k=1}^{n} \sigma_k^2 \right). \tag{10}$$

Or, alternatively, we define the approximation accuracy as

$$1 - e_w = \left(\sum_{k=1}^{w} \sigma_k^2 \right) / \left(\sum_{k=1}^{n} \sigma_k^2 \right). \tag{11}$$

Substituting equation (9) into (1) we have a compressed system model:

$$\widetilde{Y} V = \sum_{k=1}^{w} (\sigma_k \boldsymbol{u}_k)(\boldsymbol{\nu}_k^H V) \approx I \tag{12}$$

A close observation of equation (12) reveals that the set of column vectors,

$$\boldsymbol{x}_k = \sigma_k \boldsymbol{u}_k, \quad k = 1, 2, \cdots, w \tag{13}$$

form a spanning space for the injected currents I; whereas the set of complex scalars,

$$\alpha_k = \boldsymbol{\nu}_k^H V, \quad k = 1, 2, \cdots, w \tag{14}$$

can be viewed as the corresponding weight coefficient for each spanning vector.

The power flow equation of the network can be written as

$$S = V \odot I^*, \tag{15}$$

where $\odot$ means element-wise multiplication.$S = P + jQ$ is the vector of injected complex power, where

$$P = \text{Re}(V \odot I^*) = \text{VI} \cos(\angle V - \angle I), \tag{16}$$

is called the *real power* or *active power*, which equals to the DC average of the resistance component in the instantaneous power $p(t) = v(t) \odot i(t)$; whereas

$$Q = \text{Im}(V \odot I^*) = \text{VI} \sin(\angle V - \angle I) \tag{17}$$

is given the name *reactive power* because it corresponds to the component in $p(t)$ absorbed by the reactive component of the load, with zero average value and Q as its magnitude

[1] However, please be aware that the actual algorithmic implementation of most state-of-the-art SVDs (e.g. the SVD in MATLAB) does not necessarily converge to the most sensible decomposition (e.g. one as mentioned above) but a solution determined as a by-product of the computations that are used to ensure numerical stability. And the solution usually contains a rotation factor $e^{j\theta}$ in each pair of singular vectors. More explanation of the indeterminacy of SVD can be found in Appendix. For the rest of the paper, we assume that each pair of the singular vectors attained for the matrix Y are conjugate to each other.

[7]. Below we list the basic constraints for a power system to operate stably:

$$\begin{array}{ll} S = V \odot (YV)^*, & (a) \\ S_{\min} \leq S \leq S_{\max} & (b) \\ \mathrm{V}_{\min} \leq \|V\| \leq \mathrm{V}_{\max} & (c) \\ \|diag(\mathbf{y_{pr}})AV\| \leq \mathrm{I}_{\max}^{line} & (d) \\ \mathrm{Re}\left(eig(J(V))\right) \leq -\varepsilon & (e) \end{array} \tag{18}$$

(a) is for the network power flow balancing; (b) gives the input power constraints for generation or loads adjustment or power injects from other kinds of sources ; (c) represents the constraints for acceptable voltage levels; (d) is for the line thermal limits, that is, the line current $I_{line} = diag(\mathbf{y_{pr}})AV$ should keep its magnitude below some specified limit; and (e) represents the stability constraint, i.e., the Jacobian matrix of the network power flow equations,

$$J(V) = \begin{bmatrix} \frac{\partial P}{\partial \angle V} & \frac{\partial P}{\partial \|V\|} \\ \frac{\partial Q}{\partial \angle V} & \frac{\partial Q}{\partial \|V\|} \end{bmatrix}, \tag{19}$$

have negative real parts which keep a safe distance from 0. Besides the constraints mentioned above, there might be other additional constraints. Please note that the variables S, V, and Y should be taken as time-varying function, since they are changing with system operating status. Here in this section we omit the "(t)" for simplicity.

III. Compressing the Network

Applying the SVD truncation of (9) and (12) to the network power flow equation (15), we have

$$\begin{array}{rl} S \approx & V \odot \left(\sum_{k=1}^{w} \sigma_k \boldsymbol{u}_k \boldsymbol{\nu}_k^H V\right)^* \\ = & \sum_{k=1}^{w} \sigma_k{}^* \left(V \odot \boldsymbol{u}_k^*\right)\left(\boldsymbol{\nu}_k^T V^*\right) \\ = & \sum_{k=1}^{w} \alpha^* \left(V \odot \boldsymbol{x}_k^*\right), \end{array} \tag{20}$$

which we called the reduced power flow equations.

Further numerical analysis, as shown in Section V, indicates that for the network admittance matrix of an electrical power grid, not only its singular values but also each of the corresponding singular vectors, $\boldsymbol{u}_k$ and $\boldsymbol{\nu}_k$ have a small number of dominant entries. Furthermore, since the matrix Y is symmetric, each pair of the singular vectors, $\boldsymbol{u}_k$ and $\boldsymbol{\nu}_k$, are conjugate to each other. Therefore their dominant components occur at the same set of bus location. Denote by $\mathcal{N}_k$ the set of bus locations of the dominant entries in $\boldsymbol{u}_k$ and $\boldsymbol{\nu}_k$,

$$\mathcal{N}_k = \{n_k^1, n_k^2, \cdots, n_k^{c_k}\}, \tag{21}$$

which we define as the *clique*. Selecting a *clique* is done by sorting the vector entry magnitudes and setting a specific threshold on the magnitude, i.e.,

$$\begin{array}{l} \|\boldsymbol{u}_k(n_k^1)\| \geq \|\boldsymbol{u}_k(n_k^2)\| \cdots \geq \|\boldsymbol{u}_k(n_k^{c_k})\| \geq h_k \\ \|\boldsymbol{\nu}_k(n_k^1)\| \geq \|\boldsymbol{\nu}_k(n_k^2)\| \cdots \geq \|\boldsymbol{\nu}_k(n_k^{c_k})\| \geq h_k, \end{array} \tag{22}$$

with h_k being the magnitude threshold and c_k the size of the *clique*. Leave out the non-dominant entries in $\boldsymbol{u}_k$ and $\boldsymbol{\nu}_k$ by setting them to zeros, we get the truncated singular values denoted by $\widetilde{\boldsymbol{u}}_k$ and $\widetilde{\boldsymbol{\nu}}_k$, with $k = 1, 2, \cdots, w$. Therefor the network power flow equations (20) can be approximated as:

$$S \approx \sum_{k=1}^{w} \sigma_k{}^* \left(V \odot \widetilde{\boldsymbol{u}}_k^*\right)\left(\widetilde{\boldsymbol{\nu}}_k^T V^*\right) \tag{23}$$

This special structure of sparsity in an electrical power grid can be taken advantage of to conceive an efficient decentralized monitoring and control architecture. [2]

The truncated power flow equation, described as (23), implies that the system-wise power flow balancing constraints can be decentralized into a set of constrains within w *cliques*, each with c_k buses; and please note that between *cliques* there are possible overlaps. Assume that following some disturbance, a voltage discrepancy $\Delta V(t)$ is detected by the measuring or monitoring sensors, in order to bring the voltage back to its desired setting, we need to adjust the input power,

$$\begin{array}{rl} \Delta S \approx & \sum_{k=1}^{w} \sigma_k{}^* \left(V \odot \widetilde{\boldsymbol{u}}_k^*\right)\left(\widetilde{\boldsymbol{\nu}}_k^T \Delta V^*\right) \\ & +\sigma_k{}^* \left(\Delta V \odot \widetilde{\boldsymbol{u}}_k^*\right)\left(\widetilde{\boldsymbol{\nu}}_k^T V^*\right) \\ & +\sigma_k{}^* \left(\Delta V \odot \widetilde{\boldsymbol{u}}_k^*\right)\left(\widetilde{\boldsymbol{\nu}}_k^T \Delta V^*\right), \end{array} \tag{24}$$

Therefore, in order to obtain the input power adjustment as in (24), we only need to support traffic of sensor information within the clique, so that one can appropriately adjust the power to maintain the balance.

Using the identified *cliques* above, we can then design an architecture of *information highways* within an electrical power grid network based on its truncated network admittance matrix $\widetilde{Y}$ and the truncated corresponding singular vectors. Among all the *cliques*, which have *overlaps* among them, the ones with larger singular values are given higher priority to use the communication channels to send or exchange their data; within one *clique*, the sensors which corresponds to larger dominant entries in $\widetilde{\boldsymbol{u}}_k$ and $\widetilde{\boldsymbol{\nu}}_k$ are given higher priority to pass their information data. From the system-wide point of view, we see the information exchange and control actuation are implemented in a decentralized manner. Therefore it has the potential to achieve an efficient use of communication resources, avoidance of congestions, and real-time system-wide monitoring and control.

IV. Effect of Contingencies

The proposed architecture in section III reveals the decentralized coupling nature in a wide-area power grid: the buses inside a *clique* are much more strongly coupled with each other than the outside buses, except for the buses from an overlapping neighbor clique. In other words, the identification of *cliques* helps determine which generation or load settings should be adjusted in order to exert an effective impact on the power quality of some specific buses or the power flow

[2] In the following analysis, we assume a large electrical power grid network: measuring and monitoring sensors such as Phasor Measurement Units (PMUs) are available to implement across the whole network; the grid network topology and line impedances are relatively steady or changing slowly; which means that any changes of the Y matrix and the corresponding singular values and vectors can be computed or updated.

over some specific lines. On the other side, it is worth noting that the proposed coupling boundaries is drawn according to the network coupling structure, and can be very different from those by the administrative division (e.g. control zones or utility coverage boundaries). These properties makes the proposed control and communication architecture a very useful potential in applications such as real-time load shedding, generation planning, system restoration, power market operation, and etc.

One common concern is about the validity of above architecture under contingency conditions when the Y matrix undergoes some structure change, with one or more lines removed or recovered during the process. In other words, we wish to know how sensitive the SVD, as indicated in (8), is to the changes in Y when a fault occurs. Especially we are most concerned with the sensitivity of the first w singular values and the corresponding singular vectors in (9). Without loss of generality, we consider the $(n-1)$ contingency, then the corresponding change in the Y matrix can be written as

$$\begin{aligned} \Delta Y &= A(l,:)^T y_{pr}(l) A(l,:) \\ &= \begin{pmatrix} & \vdots & & \vdots & \\ \cdots & -y_{pr}(l) & \cdots & y_{pr}(l) & \cdots \\ & \vdots & \ddots & \vdots & \\ \cdots & y_{pr}(l) & \cdots & -y_{pr}(l) & \cdots \\ & \vdots & & \vdots & \end{pmatrix} \end{aligned} \tag{25}$$

Applying perturbation theory for the singular value decomposition [8] to $\widehat{Y} = Y + \Delta Y$, we have

$$\begin{aligned} &|\sigma_k(_{\widehat{Y}}) - \sigma_k(_Y)| \leq \|\Delta Y\|_2, \text{ for } k = 1:n \\ &\sqrt{\textstyle\sum_{k=1}^{n} (\sigma_k(_{\widehat{Y}}) - \sigma_k(_Y))^2} \leq \|\Delta Y\|_F \end{aligned} \tag{26}$$

where $\|\cdot\|_2$ means the Euclidean norm and $\|\cdot\|_F$ the Frobenius norm. Using (25), it gives that $\|\Delta Y\|_2 = \|\Delta Y\|_F = 2|y_{pr}(l)|$. (26) indicates that as long as $|y_{pr}(l)| \leq \epsilon$, i.e., the tripped line carries a small enough admittance, there will not be a large perturbation to the singular values.

The perturbation in the singular vectors is a little more complex to evaluate. We first need to partition the matrices as $\mathbb{U} = [U_1\ U_2]$ and $\mathbb{U} = [V_1\ V_2]$, where U_1 and V_1 consist of the first w significant left and right singular vectors respectively as shown in (9). For the post-contingency matrix, there exist $\widehat{\mathbb{U}} = [\widehat{U}_1\ \widehat{U}_2]$ and $\widehat{\mathbb{V}} = [\widehat{V}_1\ \widehat{V}_2]$ respectively. Perturbation theory gives the following combined bound for the significant singular vectors:

$$\left\| \begin{bmatrix} \widehat{U}_1 - U_1 \\ \widehat{V}_1 - V_1 \end{bmatrix} \right\|_F \leq \frac{4\|\Delta Y\|_F}{\delta_w} \tag{27}$$

where

$$\delta_w = \min_{\substack{\sigma \in \sigma(_{U_1^H Y V_1}) \\ \gamma \in \sigma(_{U_2^H Y V_2})}} |\sigma - \gamma| = \sigma_w - \sigma_{w+1}. \tag{28}$$

(27) and (28) imply that the perturbation bounds for the significant singular vectors depends on both the tripped line(s) and the approximation accuracy. If we desire $e_w \to 0$, we need to select a large $w \to n$. In this case $\delta_w \to 0$, which drives the perturbation bounds of the singular vectors to be infinity. Hence, in order to avoid frequently updating a new SVD for each contingency, we need to select an approximately smaller truncation number w. On the other hand, (27) and (28) also imply that the most significant singular vectors of Y tend to be more robust, given the same structure changes, than less-important ones, which is a desirable property for our proposed control and communication architecture.

In case that an severe contingency occurs when one important line or multiple lines get tripped (or recovered), both the singular values and the singular vectors will experience large perturbations. Therefore a new SVD has to be computed under these conditions. Fortunately the chances for severe contingencies to happen tend to be rare and the corresponding SVD(s) can be computed in advance in order to meet the real-time control and communication requirements.

V. Experiment with the NYISO-2935 System and IEEE-300 System

In this section, we experiment the SVD analysis with the NYISO-2935 system and the IEEE-300 system. This NYISO-2935 system is a representation of the New York Independent System Operator's transmission network containing 2935 nodes and 6567 links, with an average node degree of $\langle k \rangle = 4.47$. The algebraic connectivity $\lambda_2(L)$ of this network equals 0.0014215. The IEEE-300 system is a synthesized network from the New England power system and has a topology with 300 nodes and 409 links, with $\langle k \rangle = 2.73$ and $\lambda_2(L) = 0.0093838$.

Applying SVD on the Y matrix of the NYISO-2935 system, we obtain the singular values and the corresponding singular vectors. Fig. 1(a) depicts $\log(\sigma_k)$ in descending magnitude order: the curve begins with a short and sharply decreasing phase, has a long exponential phase in the middle, followed by a sharp dropping tail which finally ends at $\sigma_{\min} = 0$. (The minimum singular value is not shown in the figure in order to preserve most details in the whole plot.) Fig. 1(a) indicates that the dominant singular values decrease fast in magnitude and there should be only a small number of them. Fig. 1(b) gives the approximation accuracy $(1 - e_w)$ given the first w singular values and corresponding vectors retained in (11). It shows that when $w = 20$, the SVD approximation of Y has an accuracy of 90.33%; when $w = 35$, the approximation accuracy reaches 95%; when $w = 163$, 99%. Fig. 2 (a) and (b) present the magnitude of entries of the first 30 dominant singular vectors, $\{\boldsymbol{x}_k(s) = \sigma_k \boldsymbol{u}_k(s)\}$ and $\{\boldsymbol{v}_k(s)\}$, versus bus number s and σ order k. From this figure one can easily observe the dominant entries sparsely located in both vector groups.

Applying SVD on the Y matrix of the IEEE-300 system, we obtain its singular values and the corresponding singular vectors. Fig. 3(a) depicts $\log(\sigma_k)$ versus the σ order k, which exhibits similar descending pattern as that of the NYISO-2935 system. Fig. 3(b) gives the approximation accuracy $(1 - e_w)$ given the first w singular values and corresponding vectors

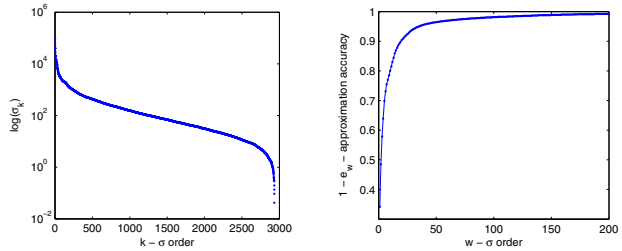

(a) (b)

Fig. 1. SVD of the NYISO-2935 system: (a) singular values σ_k versus k; (b) SVD approximation accuracy

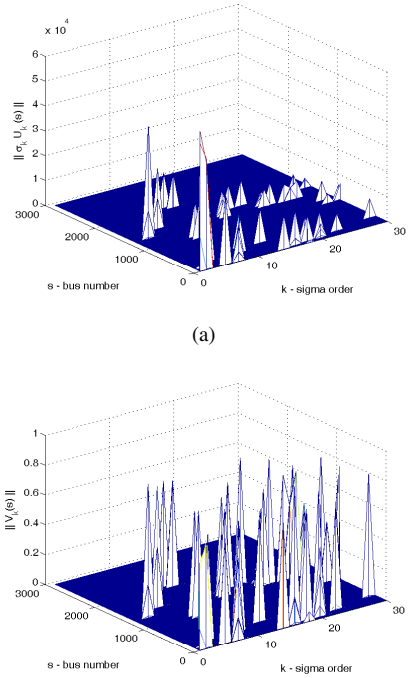

(a)

(b)

Fig. 2. The entry magnitude of dominant singular vectors: the NYISO-2935 system

retained. It shows that when $w = 8$, the SVD approximation of Y has an accuracy above 90%; when $w = 17$, it reaches 95%; when $w = 57$, 99%.

Fig. 4 shows the information highway structure of the IEEE-300 system which has 90% approximation accuracy in (11), that is, using only the first 17 most significant singular values and vectors. The entry selection threshold of the cliques, h_k, is set as

$$h_k = \gamma/\sqrt{n}, \tag{29}$$

with γ being the entry selection coefficient and $\sqrt{n}$ the normalization coefficient. In Fig.4 we experiment with the the entry selection coefficient $\gamma = 0.1$. For each clique, the source nodes, which correspond to the dominant entry locations in $\widetilde{\boldsymbol{\nu}}_k$ are marked as a group of same-color squares (with red edge and yellow fill); and the sink nodes, which

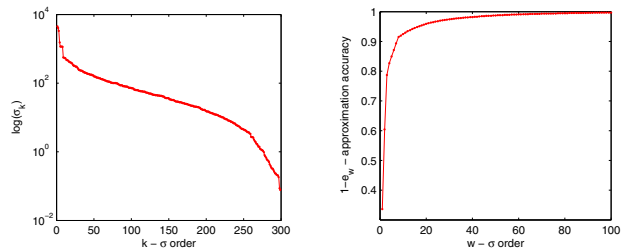

(a) (b)

Fig. 3. SVD of the IEEE-300 system: (a) singular values σ_k versus k; (b) SVD approximation accuracy

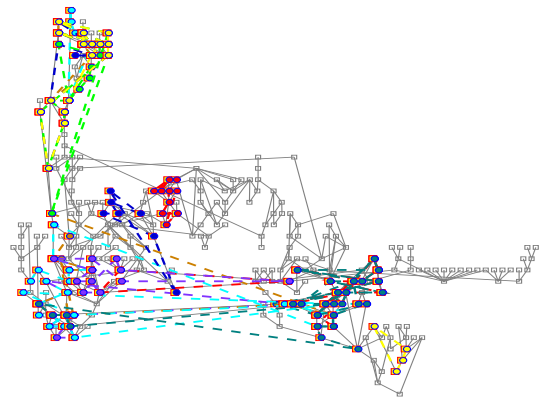

Fig. 4. The cliques in the information highway architecture of the IEEE-300 system with 90% SVD approximation accuracy of the matrix Y: the entry selection coefficient is set as $\gamma = 0.1$.

correspond to the dominant entry locations in $\widetilde{\boldsymbol{u}}_k$ are marked as a group of same-color circle dots (with black edge and a clique-distinctive color for the fill). It can be clearly seen that the sources and sinks within a clique coincides with each other. The information highways within a cliques are marked by a set of the clique-distinctive colored dashed lines which connects all the sources/sinks in it.

Table I shows the average clique size $\bar{c} = \left(\sum_{k=1}^{w} c_k\right)/w$ and the maximum clique size $c_{\max} = \max\{c_1, c_2, \cdots, c_w\}$ in the proposed *information highway* architecture for the two sample systems. The SVD approximate accuracy is set to be $1 - e_w = 90\%$. Therefore for the NYISO-2935 system, $w = 20$; for the IEEE-300 system, $w = 17$. The clique size is evaluated for different settings of γ the entry selection threshold coefficient. It can be seen that the clique size increases as we lower the entry magnitude cutting threshold. Interestingly it is found that given the same entry selection coefficient, the NYISO-2935 system has smaller clique size than the IEEE-300 system, which implies that the dominant singular-vector entries of the former are much more concentrated than the latter; which may also mean that in the NYISO-2935 system the coupling across subsystems which enclose each cliques is much weaker than that in the IEEE-300 system.

TABLE I
AVERAGE CLIQUE SIZE IN THE INFORMATION HIGHWAY ARCHITECTURE WITH THE SVD APPROXIMATION ACCURACY OF $1 - e_w = 90\%$

	$\gamma = 10^{-1}$	$\gamma = 10^{-3}$	$\gamma = 10^{-5}$	$\gamma = 10^{-7}$
$\bar{c}$: NYISO	7	16	29	51
$c_{\max}$: NYISO	17	42	74	125
$\bar{c}$: IEEE-300	13	36	73	118
$c_{\max}$: IEEE-300	29	83	159	222

VI. CONCLUSION

In this paper we apply the Singular Value Decomposition (SVD) analysis to examining the coupling structure of an electrical power grid in order to highlight opportunities for reducing the network traffic, by identifying what are the salient data that need to be communicated between parts of the infrastructure to apply a control action.

By setting the vector entry magnitude threshold, *cliques* of buses can be formed in which the implemented sensors exchange measurement data and compute the input power adjustment to in order to keep a desired operating state. Using the identified cliques, we propose a decentralized *information highway* architecture within an electrical power grid network based on its truncated network admittance matrix and the truncated corresponding singular vectors. We also discuss the potential applications of such an architecture and analyze its robustness under contingency conditions. One interesting discovery is that there exist tradeoffs between the approximation accuracy and the robustness of the compressed network model.

We then experiment the SVD analysis with the NYISO-2935 system and the IEEE-300 system and examine the proposed *information highway* architecture. Our future work will involve specific control strategies to ensure network stability.

APPENDIX

Kahaner *et al.* [9] stated that the SVD decomposition of a matrix X is unique if the singular values are distinct. However, Bro *et al.* [10] examined the SVD of a real-valued matrix $X = \mathbb{U}\Sigma\mathbb{V}^T = \sum_{k=1}^{n} \sigma_k \boldsymbol{u}_k \boldsymbol{\nu}_k^T$ and pointed out that the decomposition in fact has an intrinsic sign indeterminacy because for any pair of singular vectors, k, the following holds

$$\sigma_k \boldsymbol{u}_k \boldsymbol{\nu}_k^T = \sigma_k(-\boldsymbol{u}_k)(-\boldsymbol{\nu}_k^T). \tag{30}$$

[10] also provided a solution to the sign ambiguity problem by determining the sign of the singular vector from the sign of the inner product of the singular vector and the individual data vectors. The implementation code can be found at the MATLAB user community web site.[3]

On the other hand, we find that the results by Bro *et al.* can be generalized to complex-valued matrix with a rotation factor $e^{j\theta}$. That is, given a complex-valued matrix X, one of its SVD decomposition has $\mathbb{U}\Sigma\mathbb{V}^H = \sum_{k=1}^{n} \sigma_k \boldsymbol{u}_k \boldsymbol{\nu}_k^H$. For any pair of the singular vectors, k, it holds that

$$\sigma_k \boldsymbol{u}_k \boldsymbol{\nu}_k^H = \sigma_k(\boldsymbol{u}_k e^{j\theta})(\boldsymbol{\nu}_k e^{j\theta})^H. \tag{31}$$

which we call as the angle indeterminacy. And the sign indeterminacy in real-valued matrix SVD can be viewed as a special case of (31) with $\theta = \pi$.

In this paper, we wish to extract the conjugate singular vector pairs $\{\boldsymbol{u}_k, \boldsymbol{\nu}_k, k = 1, 2, \cdots, n\}$ of the complex-valued symmetric matrix Y from the solution of the SVD function of MATLAB. The problem of the angle indeterminacy can be solved as below:

(1) compute the angle differences between the entries in $\boldsymbol{u}_k$ and $\boldsymbol{\nu}_k$:

$$\theta_k = \angle \boldsymbol{u}_k - \angle \boldsymbol{\nu}_k^*; \tag{32}$$

(2) average the entry angle differences in θ_k:

$$\bar{\theta}_k = \text{sum}(\theta_k)/n; \tag{33}$$

(3) rotate the singular vectors to the desired directions:

$$\begin{aligned} \boldsymbol{u}_k &\Longleftarrow \boldsymbol{u}_k e^{-j\bar{\theta}_k/2} \\ \boldsymbol{\nu}_k &\Longleftarrow \boldsymbol{\nu}_k e^{-j\bar{\theta}_k/2}; \end{aligned} \tag{34}$$

ACKNOWLEDGMENT

This work was funded in part by the UIUC TCIP Project under the Grant NSF CNS 0524695, and in part by the TCIPG Project which is sponsored by the Department of Energy under Award Number DE-OE0000097.

REFERENCES

[1] A. Tiranuchit and R. J. Thomas, "A posturing strategy against voltage instabilityies in electric power systems," *IEEE Trans. on Power Systems*, vol. 3, no. 1, pp. 87–93, February 1988.

[2] A. O. Ekwue, H. B. Wan, D. T. Y. Cheng, and Y. H. Song, "Singular value decomposition method for voltage stability analysis on the national grid system (ngc)," *International Journal of Electrical Power and Energy Systems*, vol. 21, no. 6, pp. 425–432, August 1999.

[3] F. Li, "Singular value decomposition expansion for electrical demand analysis," *IMA Journal of Management Mathematics*, vol. 11, no. 1, pp. 37–48, 2000.

[4] P. Janik, J. Rezmer, P. Ruczewski, Z. Waclawek, and T. Lobos, "Adaptation of svd and prony method for precise computation of current components in networks with wind generation," in *2009 International Conference on Clean Electrical Power*, Capri, Italy, 9 – 11 2009, pp. 624 – 629.

[5] O. Krause, S. Lehnhoff, E. Handschin, C. Rehtanz, and H. F. Wedde, "On feasibility boundaries of electrical power grids in steady state," *International Journal of Electrical Power and Energy Systems*, vol. 31, no. 9, p. 437444, October 2009.

[6] Z. Wang, A. Scaglione, and R. J. Thomas, "Generating statistically correct random topologies for testing smart grid communication and control networks," *IEEE trans. on Smart Grid*, vol. 1, no. 1, Jun. 2010.

[7] J. D. Glover and M. S. Sarma, *Power System Analysis and Design, chapter 2*. Brooks/Cole, 2002.

[8] G. H. Golub and C. F. V. Loan, *Matrix Computations, chapter 8.6*. The Johns HopkinsUniversity Press, 1996.

[9] D. Kahaner, C. Moler, and S. N. S, *Numerical Methods and Software*. Upper Saddle River,NJ, USA,: Prentice Hall, 1989.

[10] R. Bro, EvrimAcar, and T. Kolda, "Resolving the sign ambiguity in the singular value decomposition," Sandia National Laboratories, Tech. Rep. SAND2007-6422, 2007.

[3] http://www.mathworks.com/matlabcentral/fileexchange/22118-sign-correction-in-svd-and-pca.